IL NUOVO CIMENTO **43 C** (2020) 107
DOI 10.1393/ncc/i2020-20107-3

COMMUNICATIONS: SIF Congress 2019

Lifetime measurement in the femtoseconds range in neutron-rich light nuclei with the AGATA tracking array

S. ZILIANI

Università degli Studi di Milano, Dipartimento di Fisica, and INFN, Sezione di Milano
Via Celoria 16, 20133 Milano, Italy

received 21 February 2020

Summary. — An extension of the Doppler-Shift Attenuation Method (DSAM) was implemented in order to perform nuclear state lifetime measurements down to tens-to-hundreds of femtoseconds in the case of complex reaction mechanisms, such as heavy-ions transfer and deep-inelastic reactions. This novel technique will have an impact in future studies of exotic neutron-rich systems produced with high-intensity radioactive ISOL-type beams. We describe here the method, in the context of an experiment realised with the aim of measuring the lifetime of excited states in neutron-rich light nuclei of C, N and O, with the combined use of the gamma detection AGATA and PARIS arrays, coupled to the VAMOS++ magnetic spectrometer in GANIL (France). The nuclei of interest were populated with low-energy transfer and deep-inelastic reactions induced by a ^{18}O beam on a thick ^{181}Ta target. As a test case for the technique validation, we show the lifetime measurement of the $1/2^-_1$ state at 3055.36(16) keV in ^{17}O: a lifetime value of $\tau = 159^{+40}_{-30}$ fs was obtained, in agreement with the literature. The impact of the excellent performance of the AGATA tracking array will be also highlighted. Finally, the new technique will be exploited to measure the lifetime of a newly discovered state in ^{18}N, at 2404.6(13) keV.

1. – Introduction

The Doppler-Shift Attenuation Method (DSAM) is a well-established technique in nuclear physics for excited states lifetime measurements in the range from 10^{-11} to about 10^{-15} s, based on a detailed investigation of the gamma-ray lineshape [1]. However, it cannot be straightforwardly applied, in its standard implementation, when the reaction-product velocity distributions in the exit channel are complex and not well defined by the reaction kinematics. This happens, for example, when heavy-ions transfer and/or deep-inelastic reactions are involved, since dissipative processes play an important role in addition to quasi-elastic mechanisms. This complex type of reactions is the only one allowing to populate yrast and near-yrast states in nuclei with large neutron excess, which

will be produced, in the future, with the employment of high-intensity radioactive ISOL-type beams [2], presently under development. Therefore, the novel implementation of the DSAM technique, here discussed, will be essential to investigate in detail the structure of exotic neutron-rich systems, including r-process nuclei, that are of key importance for nuclear astrophysics. In the following, we will concentrate on the description of the newly developed lifetime technique, focusing on light O and N nuclei produced in reactions induced by a ^{18}O beam on a thick ^{181}Ta target. Details will be given on the validation of the method considering the known experimental case of ^{17}O and on its application to a newly discovered state in ^{18}N. The importance of an excellently performing experimental set-up for gamma-spectroscopy studies, such as the advanced tracking array AGATA [3, 4], will be highlighted.

2. – Experiment

The investigation of tens-to-hundreds of femtoseconds states lifetimes in nuclei in the light neutron-rich region of the nuclear chart (*e.g.*, C, N, O) was the aim of an experiment realised in July 2017 at the Grand Accélérateur National d'Ions Lourds (GANIL) in Caen, France. A beam of ^{18}O at 126 MeV impinging on a thick ^{181}Ta target (6.64 mg/cm^2) was employed to induce direct transfer and deep-inelastic reactions to populate a variety of nuclei in the region of interest, in particular ^{16}C and ^{20}O, but also N isotopes such as ^{17}N, ^{18}N and ^{19}N.

Following the reaction, the gamma rays emitted by the excited nuclei were detected in the AGATA tracking array [3, 4], consisting of 31 segmented high-purity germanium (HPGe) detectors, coupled to the PARIS scintillation-based array [5], with two complete clusters of nine phoswich detectors each, plus two large-volume ($3.5'' \times 8''$) $LaBr_3$:Ce scintillators. The projectile-like products, which had $v/c \sim 10\%$, were detected in the VAMOS++ mass spectrometer [6], placed at the reaction grazing angle of 45°, relative to the beam direction, and with an aperture of $\Theta = \pm 6°$ and aligned with the centre of AGATA. The PARIS array was placed at 90° with respect to the VAMOS++ axis, while AGATA covered the angular range between ∼115° and ∼175°. Details on the preliminary phases of the AGATA data analysis (energy calibration and fine-tuning procedure) and on the VAMOS++ ion discrimination and velocity reconstruction are given in refs. [7] and [8], respectively.

The above-described apparatus is ideal to perform high-resolution gamma spectroscopy, together with measurements of excited-states lifetimes. In the present work, we are sensitive to lifetimes from tens to few hundreds of femtoseconds, since the target-crossing time is about 130 fs, given the target thickness of 6.64 mg/cm^2 and the projectile-like reaction products velocities of about 3 cm/ns. Gamma rays depopulating states with lifetimes significantly larger than the target crossing time will not exhibit any Doppler-shifted energy. As a matter of fact, they are emitted when the nucleus is outside the target and the fragment velocity at the time of the emission is the same as the one measured in the VAMOS++ spectrometer (such a velocity is used to perform the energy Doppler correction). On the other hand, when the depopulated excited state has a lifetime of the order of the target-crossing time, the emitted gamma rays will be Doppler-shifted, since in this case the nucleus is slowing down inside the target material and the fragment velocity is larger than the one measured afterwards in VAMOS++. In the former case, we expect narrow and symmetric gamma-ray energy peaks, while in the latter, non-Gaussian peaks, with Doppler-broadened line shapes and tails towards lower energies are observed.

The effect depends on the gamma-ray emission angle and is more prominent at backward angles.

This phenomenon discussed above is behind the excited states lifetime measurement presented in this work, that requires a comparison between the experimentally measured gamma-ray energy spectra and Monte Carlo simulated ones. To do so, we have to reconstruct the complex velocity distribution at the reaction point inside the target by unfolding the measured velocity in the magnetic spectrometer VAMOS++.

3. – Analysis procedure

The extraction of the state lifetime requires a three-step procedure, consisting of:

1) event generation;

2) AGATA simulation;

3) comparison with experimental data and χ^2 minimisation.

3˙1. *Event generation.* – In the first stage of the simulation, we generate a physics event to be passed to the subsequent AGATA simulation step. First of all, the initial fragment velocity relative to the population of a specific state has to be reconstructed. In the present experiment, the reaction mechanism is complex: the velocity distribution of the reaction products receives contributions not only from the direct population of the state of interest, but also from dissipative processes, which lead to broad structures at lower velocities (see ref. [9]). Since these dissipative contributions cannot be reliably modelled [10, 11] and we cannot consider average velocity values, as they influence the Doppler-corrected line shape from which the lifetime is extracted, we had to develop a Monte Carlo iterative procedure based on a recursive subtraction of the velocity components. In other words, we unfolded the velocity distribution measured in the VAMOS++ spectrometer.

The starting point of this procedure consists in calculating the kinetic energy of the projectile-like fragment assuming a direct population of the state of interest, having a well-defined kinematics. Then, the produced nucleus crosses the remaining thickness of the target, in which it slows down, and at the end the VAMOS++ response is applied to obtain the final velocity. After that, higher excitations of the partner and projectile-like product itself are considered, increasing the dissipated energy in 10 steps of 2 MeV each. We repeat the procedure dividing the target in 100 layers (corresponding to steps of 0.1 MeV in the beam energy), until the experimental velocity is fully described in the simulation. An example of the comparison between experimental and simulated velocity distributions is reported in fig. 1. The figure shows the velocity distribution relative to the population of the ^{17}O $1/2^-_1$ state at 3055.36(16) keV [12] which decays via the emission of a gamma ray of 2184.44(9) keV [13].

The interaction can occur with a random probability over the target thickness. The stopping power used to model the slowing down process in the target material follows the prescription given by Ziegler *et al.* in ref. [14]. The chosen stopping power assures a very good agreement between simulated and measured final velocities. The ions velocity direction in the simulation is taken directly from the measured one and introduced as a probability distribution into the Monte Carlo event generator code.

After the reaction, the excited nucleus de-excites via gamma-ray emission: the time of the gamma decay is randomly chosen on the basis of the excited-state lifetime and

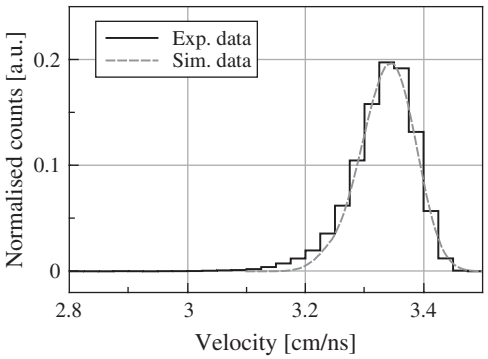

Fig. 1. – Experimentally measured (black histogram) and simulated (dashed line) velocity distribution of the ^{17}O reaction fragments, considering the population of the $1/2^-_1$ state at 3055.36(16) keV [12] which decays via the emission of a gamma ray of 2184.44(9) keV [13].

the gamma-ray Doppler correction is then performed using the ion velocity at the decay point. The gamma rays are emitted isotropically.

3˙2. *AGATA simulation.* – The events generated in the previous step are passed as input to the AGATA simulation package [15], which gives as output the gamma-ray energy deposited in the AGATA crystals. The AGATA simulation code configuration includes the 31 crystals present in GANIL during the experiment, with the corresponding geometry. After this step, the simulated data are analysed with the AGATA OFT (Orsay Forward Tracking) algorithm [16] (in the same way as experimental data are treated), in order to obtain the gamma-ray energy and the relative direction between the gamma ray and the recoiling ion. In this step, we included corrections aimed at taking into account the actual experimental energy resolution and angular distribution of the AGATA detector.

3˙3. χ^2 *minimisation.* – Once the simulation is completed, the extraction of the state lifetime requires a comparison between the experimental and simulated line shapes at different angular ranges, where the angle considered is the one between the ion direction, as measured in VAMOS++, and the emitted gamma-ray direction, as defined by the reaction point in the target and the gamma-ray interaction point in the AGATA detector. By performing the analysis of the gamma-ray line-shapes variations as a function of the angle, the procedure sensitivity significantly increases, as the line shapes depend on the angle, as explained above. The comparison is performed on the basis of χ^2, calculated varying the state lifetime and the de-exciting transition energy, which are used as parameters in the simulation. In this way, we produce a two-dimensional χ^2 lifetime-energy surface, whose minimum corresponds to the lifetime of the state with a specific transition energy. Note that in the case of lifetimes outside the method sensitivity, no localised minimum is expected, but a valley extending towards longer or shorter lifetimes should arise.

4. – Discussion

4˙1. *Technique validation.* – The technique implemented to extract the lifetimes had to be tested before being applied to unknown cases: we considered the ^{17}O and ^{19}O

nuclei as test cases. Here we will report about the ^{17}O nucleus, while details on the ^{19}O test case can be found in ref. [9], where lifetimes in both the short (∼100 fs) and the long (∼ps) ranges were investigated, considering the 2779-keV $7/2^+$ and the 2371-keV $9/2^+$ states, respectively [12].

Figure 2(a) shows the AGATA Doppler-corrected gamma-ray energy spectrum, gated on the ^{17}O reaction fragment. Three gamma-ray transitions are visible in the spectrum: $1/2^+_1 \rightarrow 5/2^+$ (g.s.) at 870.76(8) keV, $1/2^-_1 \rightarrow 1/2^+_1$ at 2184.44(9) keV [13] and $5/2^-_1 \rightarrow 5/2^+$ (g.s.) at 3842.3(4) keV [12]. The first excited state ($1/2^+_1$) has a mean lifetime $\tau = 258.6(26)$ ps [17], while the $1/2^-_1$ and $5/2^-_1$ states have lifetimes $\tau = 120^{+80}_{-60}$ fs and $\tau \leq 25$ fs [18], respectively. We are interested here in the $1/2^-_1$ state, which has a lifetime that lies in our sensitivity range.

Simulated data were produced for the 2184-keV $1/2^-_1 \rightarrow 1/2^+_1$ transition and then compared to experimental data at three angular ranges, simultaneously: 120°–140°, 140°–160° and 160°–180°. The corresponding two-dimensional χ^2 lifetime-energy surface

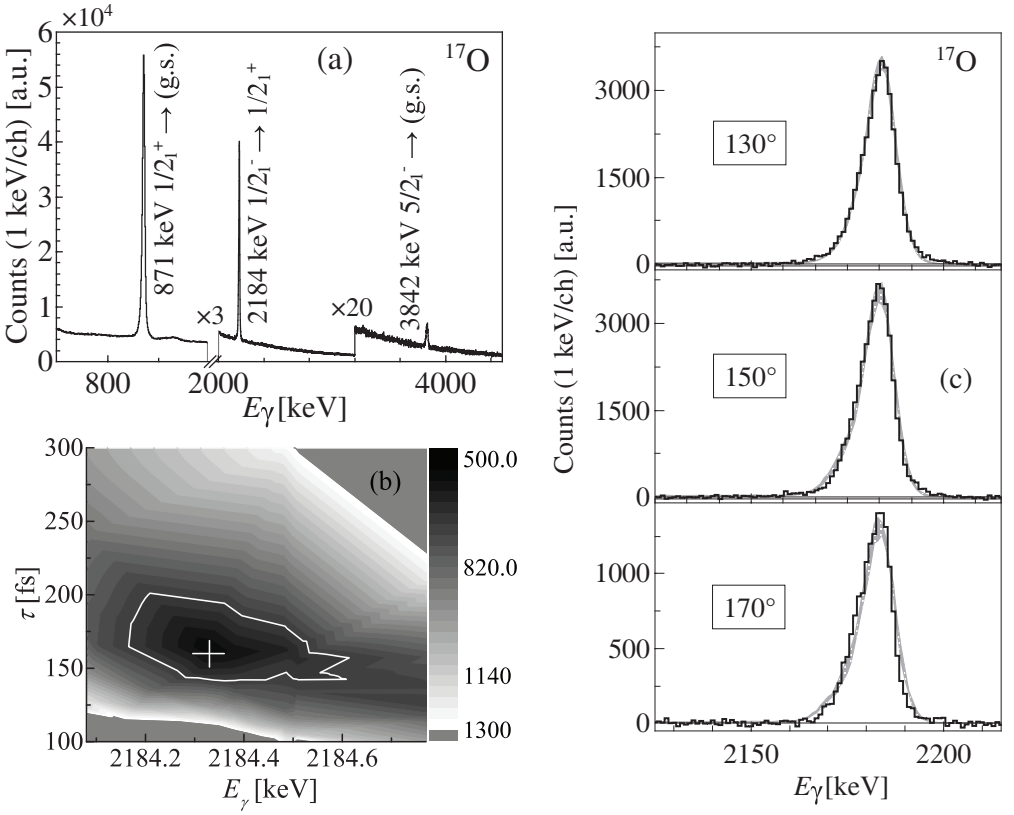

Fig. 2. – (a) AGATA Doppler-corrected ^{17}O γ-ray energy spectrum. (b) Two-dimensional χ^2 minimisation map obtained after the comparison between the measured and the simulated data for the $1/2^-_1 \rightarrow 1/2^+_1$ transition at 2184 keV in ^{17}O. The χ^2 minimum is marked with a white cross, while the white contour delimits the 1σ region. Panel (c) displays the comparison between the experimental data (black histogram) and the simulated ones within 1σ (grey bands) for three different angular ranges for the same transition considered in panel (b) (the angle reported is the mean value for each range).

is reported in fig. 2(b). As can be seen, a well-defined minimum is visible in the map: the minimum is located at $\tau = 159^{+40}_{-30}$ fs and $E_\gamma = 2184.3^{+0.3}_{-0.2}$ keV (white cross in fig. 2(b)), in agreement, within the uncertainty, with the values reported in literature of $\tau = 120^{+80}_{-60}$ fs and $E_\gamma = 2184.44(9)$ keV. Our uncertainty is obtained considering the 1σ region around the optimum value, indicated with a white contour in fig. 2(b). In fig. 2(c) the energy spectra for each angular range are overlapped with the results of the simulations within the 1σ region around the χ^2 minimum. These results, together with the ones performed for ^{19}O, validate this novel implementation of the DSAM technique.

4˙2. *AGATA sensitivity.* – The above results rely on the excellent AGATA resolution in identifying the gamma-ray first interaction point. In fact, the AGATA angular resolution is around 1°, thanks to the combined use of the Pulse Shape Analysis [19, 20] and of the tracking algorithm, which identify with a few millimetres accuracy the spatial location of energy deposit. Then, we reconstruct the energy and the direction of the interacting gamma rays, taking into account the different interaction mechanisms (photoelectric, Compton effects and pair production) that the radiation can undergo in the detection material. As VAMOS++ has an angular resolution of 1° in identifying the recoiling ions in its focal plane, the angle between the fragment velocity at the de-excitation point and the gamma-ray direction is determined with an accuracy of about 1.5°. This allows, together with a precise measurement of the ions velocity, to perform an excellent gamma-ray energy Doppler correction.

Defining the gamma-ray interaction point as the front-segment centre (see fig. 3(a)), as in conventional Ge detectors, leads to a worse Doppler correction, which affects the gamma-ray energy line shape and therefore the sensitivity to the lifetime. As a result, shallower χ^2 minima are obtained in the lifetime-energy minimisation surfaces and much larger uncertainties are achieved. As an example, fig. 3(b) displays the χ^2 minimisation surface for the same ^{17}O transition discussed before, but considering the front-segment

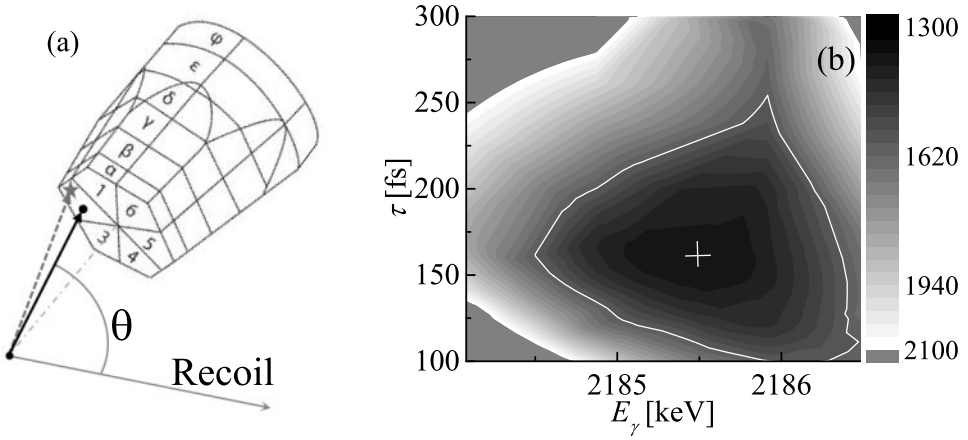

Fig. 3. – (a) Sketch of the gamma-ray emission from a recoiling reaction fragment, with real gamma interaction point (grey dashed arrow and star marker) compared to the front-segment centre (black solid arrow) in a segmented AGATA germanium detector. (b) Lifetime-energy χ^2 minimisation surface for the ^{17}O 2184-keV $1/2^-_1 \rightarrow 1/2^+_1$ transition, considering the front-segment centres as interaction points.

centres as the gamma-ray interaction points. In this case, the 1σ region is $\sim$5 times larger in energy and $\sim$2.3 in lifetime and the χ^2 value at the optimum value is $\sim$2.5 times larger than in the previous analysis.

The importance of the excellent AGATA performance is remarkably exemplified by the lifetime measurement of the 2_2^+ state in ^{20}O, which was the original goal of the experiment, with the aim of testing the predictive power of recent *ab initio* nuclear structure theories and the role of three-body forces. In ref. [21] are presented the results of the measurement: a partial lifetime for the $2_2^1 \rightarrow 2_1^+$ decay of $\tau = 190^{+102}_{-40}$ fs has been found. The result is well in agreement with the predictions from VS-IMSRG (Valence Space In-Medium Similarity Re-normalisation Group) and MBPT (Many-Body Perturbation Theory) *ab initio* calculations [22] including three-body terms (NN+NNN), but not in accordance with the value predicted with MBPT calculations in which only two-body terms (NN) have been considered (see fig. 4).

If the same analysis was performed with conventional Ge detectors (without electronic segmentation), no sensitivity would be reached, as can be seen in fig. 4. In fact, the grey band in the graph represents the uncertainty on the lifetime that would be achieved considering the gamma-ray interaction points as concentrated in the front-segment centres, leading to no sensitivity in discriminating between the different models.

4˙3. *Application to* ^{18}N. – After being validated, the previously introduced lifetime measurement technique can be applied to unknown cases, such as for example ^{18}N, which was produced in the $^{18}\mathrm{O} + {}^{181}\mathrm{Ta}$ reaction with sizeable statistics. A preliminary spectroscopic analysis can be found in ref. [23], where three new gamma transitions were observed at the energies of 1662.3(3) keV, 2073.4(8) keV and 2300.9(8) keV (see fig. 5(a)), and other two transitions around 1566 keV and 1720 keV were tentatively assigned to the same nucleus. We confirm here that the transition at 1566(1) keV comes from ^{18}N, since it is visible not only in the AGATA gamma-ray energy spectrum, but also in the

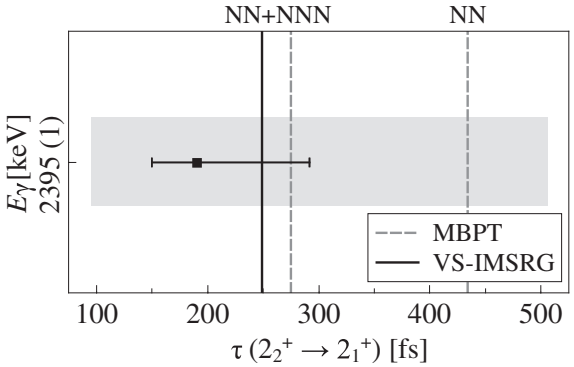

Fig. 4. – Result of the ^{20}O 2_2^+ state lifetime measurement: a partial lifetime for the $2_2^+ \rightarrow 2_1^+$ decay of $\tau = 190^{+102}_{-40}$ fs has been found [21], and is here marked with the black square. The result is in agreement with both VS-IMSRG (solid line) and MBPT (dashed line) *ab initio* calculations [22] including two- and three-body forces (NN+NNN), while no accordance can be found with MBPT considering two-body terms only. The grey band represents the uncertainty that would be reached using traditional germanium detectors (*i.e.*, without electronic segmentation), here simulated considering the gamma-rays interactions as concentrated in the front-segment centres of the AGATA segmented crystals.

PARIS scintillator array placed at 90° with respect to the recoiling direction. This makes it possible to firmly exclude contaminants contributions to the gamma spectrum. Regarding the peak observed at 1720 keV, its assignment is still not firm, due to the lack of statistics in both the AGATA and PARIS spectra. Reference [23] quotes a new excited state at the energy of 2403.5(3) keV, with the constraint that no lifetime effect was taken into account in the reconstruction of the level scheme. In the present paper we give, for the first time, an estimate to the lifetime of this newly discovered state, measured with the previously introduced technique, and in fig. 5(b) we present an updated version of the level scheme, with the energies corrected for the effects of short excited-states lifetimes, where needed.

We realised simulations for the 1662-keV transition, de-exciting the newly discovered state, and then we performed a comparison between the simulated and experimental data for the total spectrum, *i.e.*, with all the angles between the recoil and gamma-ray directions summed up. Unlike the case of ^{17}O previously discussed, we could not split the energy spectrum in three angular ranges due to the limited statistics. The corresponding χ^2 lifetime-energy surface is reported in fig. 6(a): a global minimum is present in the map at $\tau = 160^{+740}_{-100}$ fs and $E_\gamma = 1663.0(8)$ keV. The comparison between the simulated data and the background-subtracted experimental spectrum is reported in fig. 6(b), where the grey band corresponds to the 1σ region.

Regarding the 1σ region, the transition energy is well constrained, while the lifetime error bar extends quite largely towards longer lifetimes, even though the region is still confined. This effect can be imputed to the lack of statistics and to the fact that the analysis cannot be performed for different angular ranges, losing part of the sensitivity to the lifetime, although we cannot exclude a lifetime value of several hundreds of femtoseconds. Given the above transition energy, we can extract a more precise value for the energy of the newly discovered state, *i.e.*, $E_{level} = 2404.6(13)$ keV. Note that this value is obtained considering the energy of the $(3^-) \rightarrow (2^-_1)$ transition to be 627(1) keV, as quoted by Wiedeking *et al.* in ref. [24], in order to avoid any lifetime effect of our energy measurements, *i.e.*, Doppler shifted energies (see sect. **2** for details). The

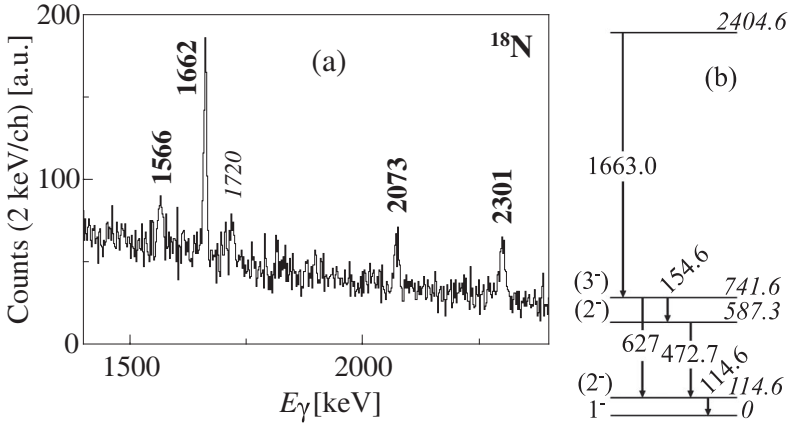

Fig. 5. – (a) Partial AGATA Doppler-corrected ^{18}N γ-ray energy spectrum: the transitions in bold are assigned to the nucleus, while the 1720-keV peak (in italics) assignment is not certain due to limited statistics. (b) Updated version of the ^{18}N nucleus level scheme of ref. [23], considering lifetime effects (see text for details and error bars).

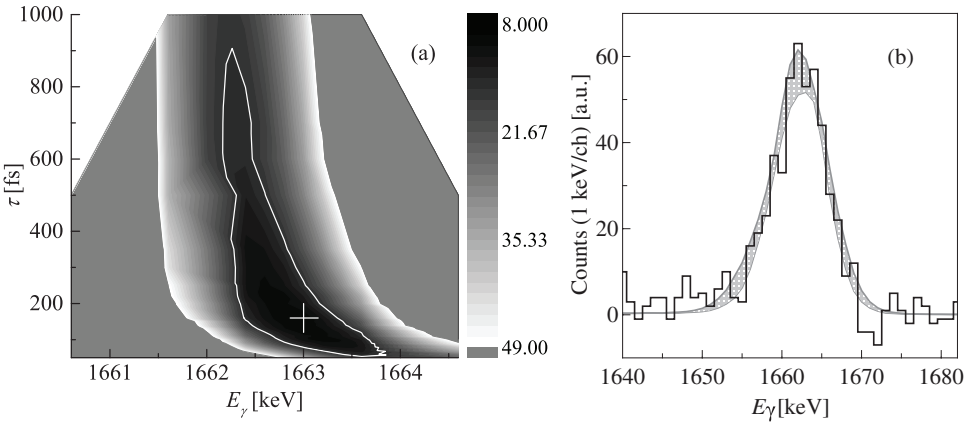

Fig. 6. – (a) Lifetime-energy χ^2 minimisation surface for the ^{18}N 1663-keV transition. The minimum is indicated by the white cross, while the solid white contour delimits the 1σ region. (b) Comparison between the background-subtracted experimental data (black histogram) and the simulated ones within 1σ (grey band) for the same 1663-keV transition considered in panel (a).

$(2^-_1) \rightarrow g.s.$ transition energy considered is the one measured in the present work, *i.e.*, $E_\gamma = 114.6(1)$ keV, since the lifetime of the first excited (2^-) state is quoted to be of $\tau = 582(165)$ ps from recoil-distance measurements in ref. [24], therefore the energy measurement is not affected. For completeness, the energy of the second (2^-) excited state reported in fig. 5(b) ($E_{level} = 587.3(2)$ keV) was obtained considering the $(2^-_2) \rightarrow (2^-_1)$ transition energy quoted in ref. [25] to be $E_\gamma = 472.7(2)$ keV: our value is in agreement with the one quoted in the literature [12]. In the level scheme we report also the $(3^-) \rightarrow (2^-_2)$ transition, previously observed by Wiedeking *et al.* in ref. [24] at 155 keV, and present also in the current experiment at the energy of 154.6(3) keV. This transition is hardly visible in the total energy spectrum due to the presence of a Doppler-smeared partner gamma-ray contaminant, but in the angular range of 120°–140°, the contaminant line moves to lower energies and the ^{18}N peak becomes clearly visible.

Finally, we note that no spin assignments were investigated thus far and the reported ones are taken from the database [12]. In addition, no comparison with theory is available, yet, for the newly introduced state and its lifetime, as discussed in details in ref. [23].

5. – Conclusions

A novel implementation of the DSAM lifetime-measurement technique was presented. This technique allows to measure lifetimes in the range from tens to hundreds femtoseconds using reactions with a complex initial velocity distribution, as in the case of heavy-ions transfer and deep-inelastic processes. The new technique was tested with known excited-state lifetimes in ^{17}O and ^{19}O, obtaining a good agreement with literature values. The reliability of the results depends largely on the excellent performance of the experimental apparatus, in particular the AGATA array, without which a very limited sensitivity to the lifetimes would be achieved. The technique was used to investigate the unknown case of a newly discovered state in ^{18}N, for which the lifetime $\tau = 160^{+740}_{-100}$ fs and the corresponding de-exciting transition energy $E_\gamma = 1663.0(8)$ keV were obtained. Considering the lifetime effects, *i.e.*, Doppler shifted energies, the energy of the state was calculated to be $E_{level} = 2404.6(13)$ keV.

The presently described DSAM implementation will play a significant role in the investigation of exotic neutron-rich nuclei, that will be populated in the near future with the use of intense radioactive ISOL-type beams [2], *e.g.*, at ISOLDE-CERN [26], SPIRAL2 at GANIL [27] and SPES [28] at the Legnaro National Laboratory of the italian Istituto Nazionale di Fisica Nucleare.

* * *

I thank S. Leoni, B. Fornal, M. Ciemała and F. C. L. Crespi for their contributions to this project and the AGATA-PARIS-VAMOS Collaboration for the realisation of the experiment. This work was supported by the Italian Istituto Nazionale di Fisica Nucleare, by the Polish National Science Centre under Contract No. 2014/14/M/ST2/00738, 2013/08/M/ST2/00257 and 2016/22/M/ST2/00269, and by RSF Grant No. 19-42-02014. This project has received funding from the European Union's Horizon 2020 research and innovation programme under grant agreement No. 654002.

REFERENCES

[1] Alexander T. K. and Forster J. S., *Adv. Nucl. Phys.*, **10** (1978) 197.
[2] Köster U., *Eur. Phys. J. A*, **15** (2002) 255.
[3] Akkoyun S. *et al.*, *Nucl. Instrum. Methods Phys. Res. A*, **668** (2012) 26.
[4] Clément E. *et al.*, *Nucl. Instrum. Methods Phys. Res. A*, **855** (2017) 1.
[5] Maj A. *et al.*, *Acta Phys. Pol. B*, **40** (2009) 565.
[6] Rejmund M. *et al.*, *Nucl. Instrum. Methods Phys. Res. A*, **646** (2011) 184.
[7] Ziliani S. *et al.*, *Acta Phys. Pol. B*, **50** (2019) 625.
[8] Ciemała M. *et al.*, *Acta Phys. Pol. B*, **50** (2019) 615.
[9] Ciemała M. *et al.*, *Acta Phys. Pol. B*, **51** (2020) 699.
[10] Zagrebaev V. I., Fornal B., Leoni S. and Greiner W., *Phys. Rev. C*, **89** (2014) 054608.
[11] Karpov A. V. and Saiko V. V., *Phys. Rev. C*, **96** (2017) 024618.
[12] National Nuclear Data Center, `https://www.nndc.bnl.gov/`.
[13] Firestone R. B. and Revay Zs., *Phys. Rev. C*, **93** (2016) 044311.
[14] Ziegler J. F., Biersack J. P. and Littmark U., *The Stopping Power and Range of Ions in Solids*, Vol. **1** (Pergamon Press, New York) 1984.
[15] Labiche M. *et al.*, AGATA GEANT4 Simulations for AGATA@GANIL, `http://npg.dl.ac.uk/svn/agata/`.
[16] Lopez-Martens A., Hauschild K., Korichi A., Roccaz J. and Thibaud J. P., *Nucl. Instrum. Methods Phys. Res. A*, **533** (2004) 454.
[17] Ajzenberg-Selove F., *Nucl. Phys. A*, **166** (1971) 1.
[18] Alexander T. K., Broude C. and Litherland A. E., *Nucl. Phys. A*, **53** (1964) 593.
[19] Venturelli R. and Bazzacco D., LNL annual Report No. 2004.
[20] Bruyneel B., Birkenbach B. and Reiter P., *Eur. Phys. J. A*, **52** (2016) 70.
[21] Ciemała M. *et al.*, *Phys. Rev. C*, **101** (2020) 021303(R).
[22] Hebeler K., Holt J. D., Menéndez J. and Schwenk A., *Annu. Rev. Nucl. Part. Sci.*, **65** (2015) 457.
[23] Ziliani S. *et al.*, *Acta Phys. Pol. B*, **51** (2020) 709.
[24] Wiedeking M. *et al.*, *Phys. Rev. C*, **77** (2008) 054305.
[25] Pravikoff M. S. *et al.*, *Nucl. Phys. A*, **528** (1991) 225.
[26] ISOLDE, CERN, `https://isolde.web.cern.ch/`.
[27] GANIL-SPIRAL2, `https://www.ganil-spiral2.eu/`.
[28] SPES Project, `https://web.infn.it/spes/`.